Electromagnetic design and optimization of a superconducting quarter wave resonator *

YANG Liu(杨柳)[1,2] LU Xiang-Yang(鲁向阳)[1;1)] QUAN Sheng-Wen(全胜文)[1]
YAO Zhong-Yuan(姚中元)[1] LUO Xing(罗星)[1] ZHOU Kui(周奎)[1]

[1] State Key Laboratory of Nuclear Physics and Technology, Peking University, Beijing 100871, China
[2] Institute of Fluid Physics, Chinese Academy of Engineering Physics, Mianyang 621900, China

Abstract: Superconducting (SC) cavities currently used for the acceleration of protons at a low velocity range are based on half wave resonators. Due to the rising demand on high current, the issue of beam loading and space charge problems has arisen. Qualities of low cost and high accelerating efficiency are required for SC cavities, which are properly fitted by using an SC quarter wave resonator (QWR). We propose a concept of using QWRs with frequency 162.5 MHz to accelerate high current proton beams. The electromagnetic design and optimization of the prototype have been finished at Peking University. An analytical model derived by the transmission line theory is used to predict an optimal combination of the geometrical parameters, with which the calculation by Microwave Studio shows a good agreement. The thermal analysis to identify the temperature rise of the demountable bottom plate under various levels of thermal contact also has been done, and the maximum increment is less than 0.5 K even though the contact state is poor.

Key words: high intensity proton beam, superconducting quarter wave resonator, demountable plate

PACS: 29.20.Ej **DOI:** 10.1088/1674-1137/37/2/027001

1 Introduction

Low β (relativistic velocity, $\beta = v/c$) superconducting (SC) cavities, boosted by increasing interest in the high intensity proton beam sources, have been developed worldwide [1]. With different geometries, frequencies, and gap numbers, a large number of resonators have been built for a variety of applications [2–5]. A 10 mA, 50 MeV superconducting proton linac as the demo of Chinese Accelerator Driven System driver has recently been designed and constructed [6]. Its injector part consists of a normal conducting radio frequency quadrupole with output energy 2.1 MeV and an SC linac enhancing beam energy up to 10 MeV. Two types of frequency, 162.5 MHz and 325 MHz, are chosen to ensure technical feasibility. The referred accelerating structures include the crossbar H mode (CH) cavity and half wave resonator (HWR) with frequency 162.5 MHz, and 325 MHz spoke cavity. Since increasing beam current poses an issue of beam loading and space charge problems, cavities with low cost and high accelerating efficiency are preferred. Instead of these half wave resonators, the quarter wave resonator (QWR) with frequency 162.5 MHz presents better performances in fulfilling the requirements of cost and efficiency, thus making it a possible alternative for the injector linac.

The frequency of 162.5 MHz is much higher than that of the SC QWRs for heavy ions, which are generally under 100 MHz. As a result, the cavity size is reduced a great deal, and the mechanical properties of SC QWR are significantly improved. In the case of the same designed β, a QWR provides a double sized effective accelerating length as spoke cavities and HWRs are mostly applied in frequencies above 300 MHz, while their cavity sizes are comparable. In terms of an HWR with identical frequency, it would require a larger sized cryomodule, which causes higher static and dynamic heat loss. Since an HWR needs twice the energy content for the same cavity voltage, it shows less efficiency on power utility. Lower fabrication cost is another essential point benefiting from the reduced cavity size and also simple geometry, especially compared with the CH type cavity. In addition, a QWR is capable of using demountable end plate instead of electron beam welding, where the surface current density is sufficiently low. This unique characteristic for SC QWRs, enables a convenient access for surface processing, and plays an important role in the improvement of quality factor [7].

Received 16 March 2012
∗ Supported by Major Research Plan of National Natural Science Foundation of China (91026001)
1) E-mail: xylu@pku.edu.cn

The main factor limiting SC QWR to accelerate apply for high current proton beam is the beam steering caused by an up-down asymmetry with respect to the beam axis, which is absent for half wave resonators [8]. However, numerical calculations suggest that the steering of the particular QWR with frequency 162.5 MHz can be greatly reduced at a wide β range by an applicable method. More details are referred to in the study of the feasibility of using SC QWR for accelerating a high intensity proton beam [9]. The following sections will focus on the electromagnetic design and optimization of the QWR. The designed $\beta_{\rm G}$ is 0.085, which ensures the proton beam will always obtain the maximum energy gain at the energy range 2.1–10 MeV.

2 The design target

A very high gradient is not required by the applications of a low velocity proton beam for reliable acceleration. Therefore, the RF parameters standing for peak surface fields, namely, $E_{\rm p}/E_{\rm acc}$ and $B_{\rm p}/E_{\rm acc}$, would not be extremely pursued, but merely ensure that the QWR still operates at a safe point even with the highest gradient, 8 MV/m. The parameters dominantly determining the level of cost and efficiency for the cavity should be primarily considered. Quality factor (Q_0) and the ratio (shunt impedance over Q_0, R/Q_0) significantly affect the load of the cryogenic system and the efficiency of the cavity delivering energy to beams, respectively. Both of them should be as high as possible. Instead of the definition of Q_0, it can be expressed by another form: Q_0=$G/R_{\rm s}$, where G is the geometry factor and $R_{\rm s}$ is the surface resistance of a cavity [10]. Maximizing G and minimizing $R_{\rm s}$ are the key solutions to the improvement of Q_0. The former one can be done in the stage of electromagnetic optimization, while the latter one is greatly influenced by the quality of the surface processing, for which the end plate of the QWR would be demountable. The effective accelerating length, as another important parameter for cavity design, is unchangeable when the frequency and designed $\beta_{\rm G}$ are confirmed, and is not in the optimizing parameter list.

3 The model setup

An initial model of the QWR was set up, as shown in Fig. 1. Some general considerations about easy fabrication and mechanical stability made the model approach a simple geometry. As a result, the beam tube areas are in the shape of a cone but not the typical 'donut', which has been frequently adopted [11, 12], yet the middle drift tube seems like a donut to evenly distribute the surface electric field. The inner conductor has larger diameter at the shorting end (d) not only to reduce the surface magnetic field, but also to weaken its mechanical vibrating response to the external stimulation. For the same reason, a sphere-shell structure with better mechanical stability becomes the connection between the inner and outer conductors. In order to lower the surface current down to a safe level ($B_{\rm c}/E_{\rm acc}$ <0.1 mT/(MV/m) [12]) for the non-welded contact region of the demountable plate, the vertical distance from there to the beam axis (h) was adjusted to a proper value. The beam aperture was set at 40 mm to reduce the beam loss. The diameter of the outer conductor (D) is approximately equal to $\beta_{\rm G}$ λ, where λ is the wavelength of the RF field. The length between the beam tube top faces (L) can also be initially determined since the transit time factor at $\beta_{\rm G}$ generally gets to its maximum when L is about equal with $(2\beta_{\rm G}\lambda)/3$ [13].

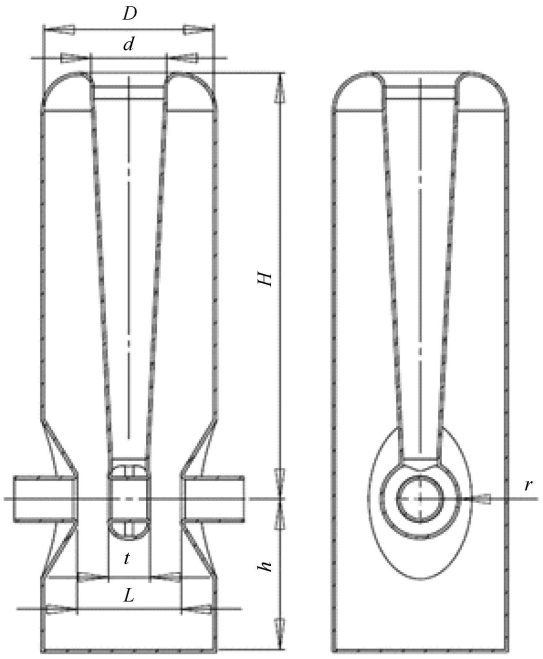

Fig. 1. Cut views of the QWR model.

4 The transmission line approximation

A QWR is approximately equivalent to a capacitance-loaded quarter wave coaxial transmission line. Using the transmission line theory, the analytical solutions of the concerned RF parameters strongly depending on cavity geometry can be obtained. As the bottom plate is far away from the inner conductor open end, the loaded capacitance is reasonably neglected. Defining ρ as the ratio of the radius of the inner conductor over that of the outer one, we can have the formulas associated with the peak surface fields:

$$\frac{E_{\rm p}}{E_{\rm acc}}=\frac{1}{\rho\ln\left(\frac{1}{\rho}\right)}, \tag{1}$$

and

$$\frac{B_{\rm p}}{E_{\rm acc}}=\sqrt{\mu_0\varepsilon_0}\frac{1}{\rho\ln\left(\frac{1}{\rho}\right)}, \tag{2}$$

where μ_0 is the permeability in a vacuum space, and ε_0 the permittivity. The transit time factor has been assigned with constant 1 for the derivation of the gradient $E_{\rm acc}$, which is much higher than the real case, and the difference is rather appreciable in the low ρ range, typically less than 0.4. In terms of the geometry factor G and R/Q_0, they present as:

$$G=\pi\sqrt{\frac{\mu_0}{\varepsilon_0}}\beta_{\rm G}\frac{\ln\left(\frac{1}{\rho}\right)}{1+\frac{1}{\rho}}, \tag{3}$$

and

$$\frac{R}{Q_0}=\frac{16}{\pi}\sqrt{\frac{\mu_0}{\varepsilon_0}}\ln\left(\frac{1}{\rho}\right). \tag{4}$$

Equation (3) suggests that the geometry factor G is a function directly proportional to the designed $\beta_{\rm G}$, which obviously explains the phenomenon that the Q_0 of low β SC cavities is generally lower than that of the high β ones. More importantly, G is not influenced by the error of the gradient $E_{\rm acc}$, and can be used to evaluate the results of optimization. These properties can be summarized in a plot (Fig. 2). For clarity, all the RF parameters are transformed into dimensionless quantities and scaled to the same order. As is seen from the plot, both $E_{\rm p}/E_{\rm acc}$ and $B_{\rm p}/E_{\rm acc}$ get to a minimum as $\rho\approx0.4$, while G is maximized when ρ reduces to 0.3. They are unable to be optimized simultaneously, thus, a tradeoff should be taken into account during the optimization procedure. As for R/Q_0, it is partly determined by the voltage at the open end, which is essentially induced by the varying rate of the magnetic flux crossing the area between the inner conductor and the outer one. Smaller radius of the inner conductor definitely leads to larger R/Q_0.

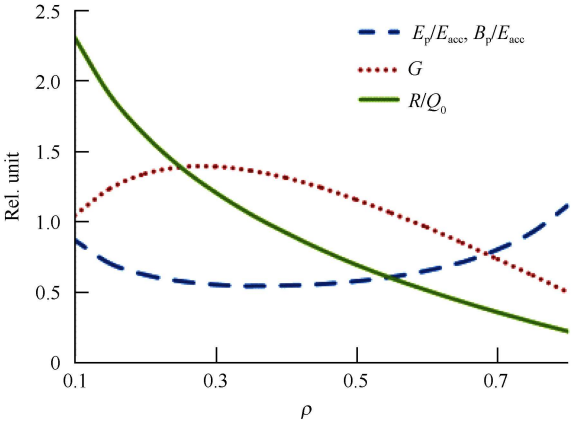

Fig. 2. The dimensionless RF parameters as functions of ρ.

5 Optimization

It seems that these uncertain geometrical parameters shown in Fig. 1 can be immediately predicted by the above analysis. As the geometry factor G and R/Q_0 are the primary concern, ρ should be assigned to 0.3 or a little bit lower. Nevertheless, the mechanical stability calls for a larger inner conductor, otherwise, its vibrations forced by external stimulation would occur easily, and they should be thoroughly eliminated. The balanced results are like this: d=0.45D, t=0.4L, $2r$=0.45D. Importing the defined model into the software-Microwave Studio (MWS), all the RF parameters were calculated, and listed in Table 1. The accuracy was improved by refining the mesh size and a large number of mesh, almost 1 million, was generated. According to Eq. (3), substituting $\beta_{\rm G}$=0.085, we get $G_{\rm max}$=28, corresponding to ρ=0.3, and it is the best result that we can ever achieve as long as the designed $\beta_{\rm G}$ is ensured. The simulation result gets very close to $G_{\rm max}$, which indicates that these geometrical parameters are well optimized. In terms of the peak surface fields, when the gradient $E_{\rm acc}$ gets to 8 MV/m, $E_{\rm p}$ and $B_{\rm p}$ will be 46.4 MV/m, 70.4 mT, which are still acceptable.

Table 1. The optimized RF parameters.

$E_{\rm p}/E_{\rm acc}^{1)}$	$B_{\rm p}/E_{\rm acc}$/(mT/(MV/m))	G/Ω	$R/Q_0/\Omega$	$B_{\rm c}/E_{\rm acc}$/(mT/(MV/m))
5.8	8.8	27.6	407	0.045

1) $E_{\rm acc}$ is calculated with the effective length $\beta_{\rm G}\lambda$.

6 Thermal analysis for the demountable plate

In the operating mode, the demountable plate will not be directly cooled by liquid helium (LHe). All the heat generated on the plate is conducted away through the contact region between the plate and the main cavity wall. To study the temperature rise on the plate in various contact states, a thermal analysis has been done by ANSYS [14]. The thermal conductivities of niobium (the residual resistance ratio is about 300) at low temperature around 4.2 K are from Ref. [10]. The advanced contact method was used, and the contact thermal conductivity was assigned with a reduced factor (α) by the thermal conductivity of niobium. The factor is variable to adapt the different contact situations from bad to perfect, corresponding to a range of 0.01∼1. The boundary cooled by LHe was constrained at a constant temperature 4.2 K. Heat loads were applied on the surfaces where the tangent component of the magnetic field is non zero, and under the worst condition of $E_{\rm acc}$=8 MV/m, $R_{\rm s}$=100 nΩ (the BCS theory predicted resistance $R_{\rm BCS}$=10 nΩ). As a temperature dependent quantity, $R_{\rm BCS}$ increases with

the temperature rise, which reversely introduces more heat load and increases the temperature in a positive feedback way. During the calculation, the procedure would be iterative until the final steady state is found. A simpler alternative way is adopted: set $R_{\rm BCS}$=20 nΩ, while the consistent temperature is 5 K, thus a reasonable convergence would be reached as long as the maximum temperature is lower than 5 K, see Fig. 3. A sharp temperature rise occurs because of bad contact when the factor α is less than 0.1, but is affordable yet as α reduces down to 0.01. In reality, to improve the contact quality, a gasket can be adopted as a seal in the contact region, such as pure lead (above 99.99% of Pb), which superconducts at 4.2 K and is soft enough to be largely deformed.

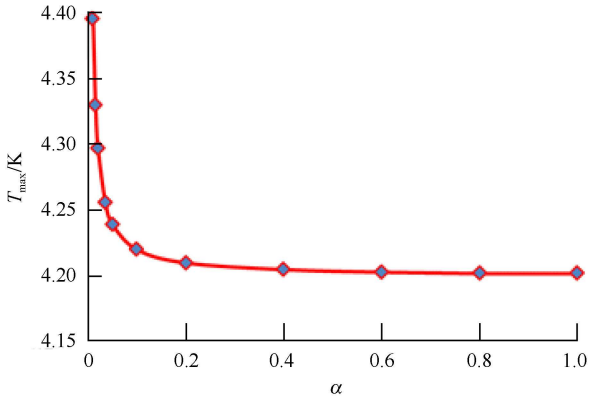

Fig. 3. The maximum temperature ($T_{\rm max}$) on the demountable plate versus different contact situation.

7 Conclusion

The MWS simulation of the QWR reveals relatively low peak surface field ratios of $E_{\rm p}/E_{\rm acc}$=5.8, and $B_{\rm p}/E_{\rm acc}$=8.8 mT/(MV/m). The geometry factor G almost gets to the maximum predicted by the analytical method, which suggests the foundation of the possible optimal combination of the geometrical parameters. The QWR also has sufficient low current at the surface of the demountable plate. This property guarantees that only a small amount of heat can be induced on the plate and the temperature rise predicted by ANSYS is within the safe range. Hence, the use of a demountable plate at the bottom end of the QWR is feasible and advisable, as the improvement of the quality factor Q_0 also depends on the performance of the surface processing in addition to the electromagnetic optimization.

References

1 Facco A et al. Low and Medium Beta SC Cavities. Proc. EPAC, 2004
2 Devanz G. Superconducting RF Technology for Proton and Ion Accelerators, Proc. IPAC2011
3 Mosnier A. The IFMIF 5 MW Linacs. Proc. LINAC, 2008
4 Ristori L et al. Design, Fabrication and Testing of Single Spoke Resonators at Fermilab. Proc. SRF, 2009
5 Dziuba F et al. Development of Superconducting CH-Cavities for the Eurotrans Injector Linac. Proc. SRF, 2009
6 HE Y et al. The Conceptual Design of Injector II of ADS in China. Proc. IPAC, 2011
7 Andreev V et al. Physical Review Special Topics-Accelerators and Beam, 2003, **6**: 040101
8 Ostroumov P N, Shepard K W. Physical Review Special Topics-Accelerators and Beam, 2001, **4**: 110101
9 YANG L et al. Chinese Physics C, 2012, **36**(11): 1116–1119
10 Hasan Padamsee et al. RF Superconductivity for Accelerators. John Wiley & Sons, INC., 1998, 129–143
11 Kelly M P et al. Superconducting 72 MHz beta=0.077 Quarter-Wave Cavity for ATLAS Proc. PAC, 2011
12 Laxdal R E et al. Production and Testing of Two 141 MHz Prototype Quarter Wave Cavities for ISAC-Ⅱ. Proc. LINAC, 2008
13 Delayen J R. Low and Intermediate Beta Cavity Design – a Tutorial. Proc. SFR, 2007
14 http://www.ansys.com/products/multiphysics.asp